Supplementary Information for

Mechanistic Insights into Passive Membrane Permeability of Drug-Like Molecules from a Weighted Ensemble of Trajectories

She Zhang[1], Jeff P. Thompson[1], Junchao Xia[1], Anthony T. Bogetti[2], Forrest York[1], A. Geoffrey Skillman[1], Lillian T. Chong[*,2], David N. LeBard[*,1]

[*] To whom correspondence should be addressed

[1]OpenEye Scientific, Santa Fe, NM 87508
[2]Department of Chemistry, University of Pittsburgh, Pittsburgh, PA 15260

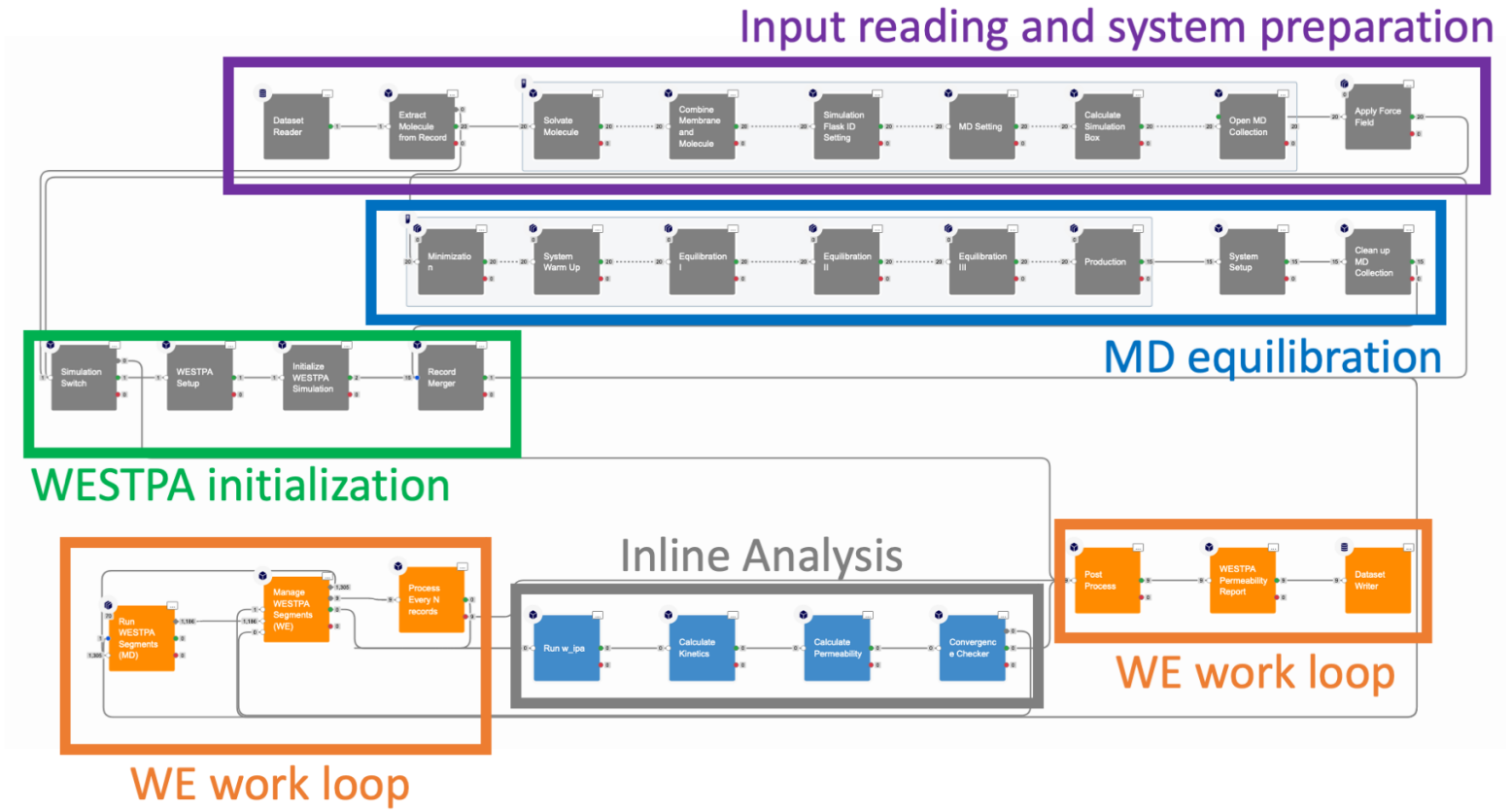

Figure S1. Structural layout of the OpenEye Permeability Floe, which can be broken into 5 logical phases: (1) Preparation of input the permeate system (purple); (2) Equilibration using a standard MD protocol of the aqueous ligand/membrane system (blue); 3) Initialization of the WESTPA toolkit (green); (4) Loop of segment trajectory splitting/recycling events using the WE algorithm, and output trajectory storage (orange); (5) Inline analysis of the permeability simulation for kinetics and convergence criteria (gray).

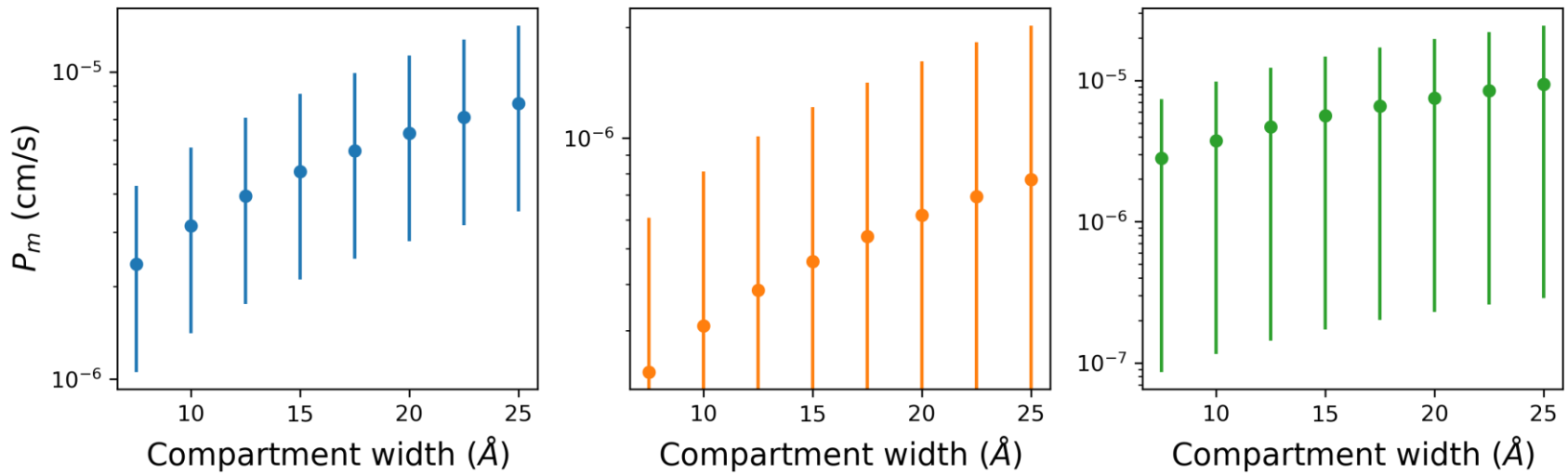

Figure S2. The estimated permeability as a function of the compartment width. The upper limit, 25 Å, is the full length of the water compartment in our simulation ($(L_z - 40\text{Å})/2$). The lower limit, 7.5 Å, roughly corresponds to the thickness of the water layer near the membrane surface.

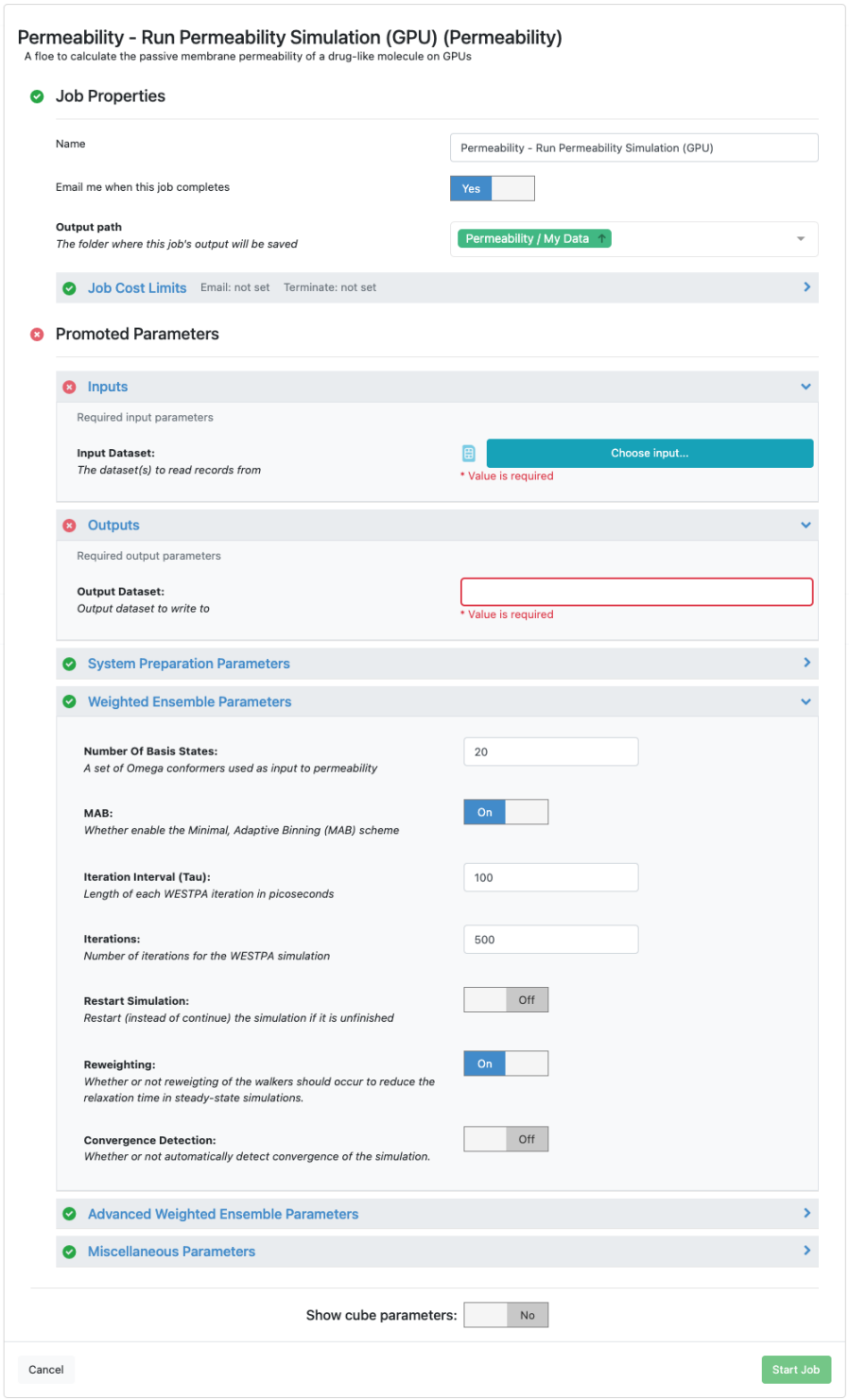

Figure S3. The Floe setup GUI of the OpenEye Permeability Floe. All the parameters have a brief description of their function and are grouped with other parameters of the same component (e.g., system preparation, WE simulation, etc.) for easier navigation on the user's end.

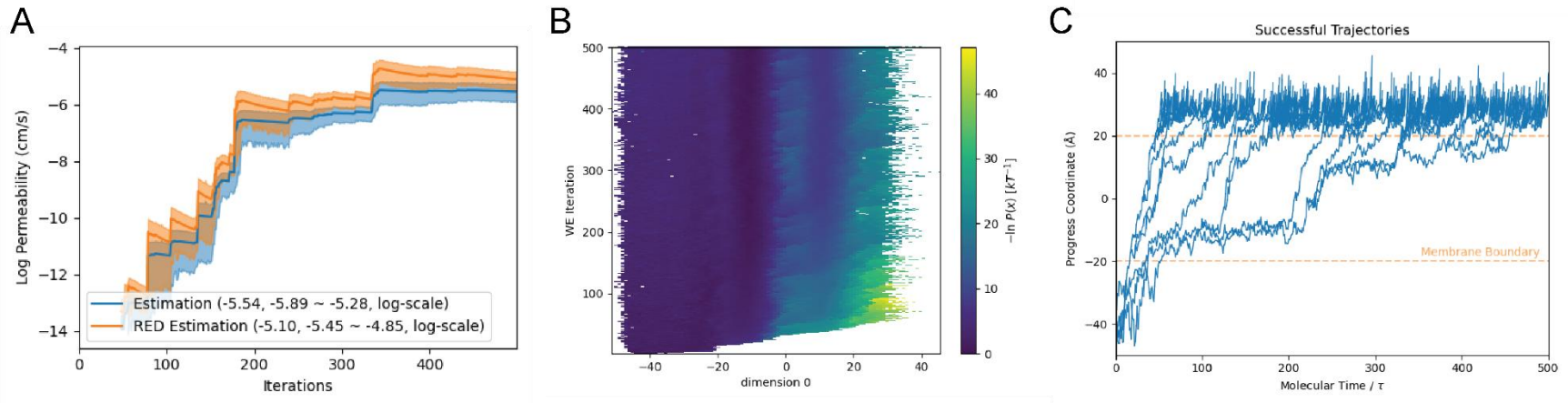

Figure S4. Simulation report figures generated by OpenEye Permeability Floe. A) The time (iteration=molecular time/τ) evolution of the permeability estimate (*blue*) and that estimated using RED (*orange*). The curves represent the mean estimates, and the shaded areas represent 95% CI. **B)** The time evolution of the probability distribution (in units of $k_B T$). **C)** All the recycled trajectories in the regular WE with fixed binning scheme run represented by the progress coordinate, *z* (y-axis), versus the molecular time in terms of the number of iterations (x-axis).

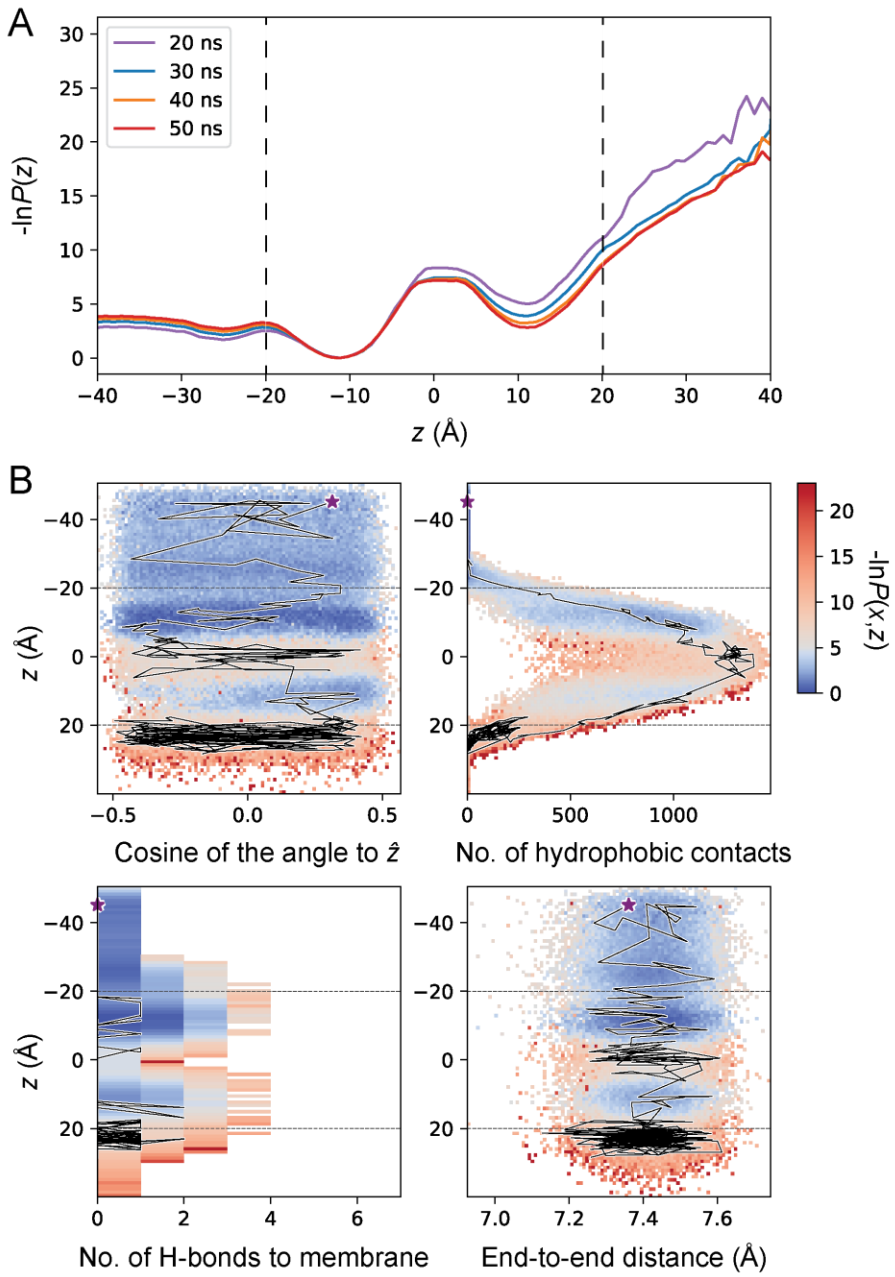

Figure S5. The original, unsymmetrized (inverted) probability distribution along the lipid normal ($\hat{z}$) for tacrine using the reweighting WE protocol (WESS). Note that, due to the recycling condition imposed by the WE steady-state protocol, this is not a free energy profile. See Figure 3 legend for details.

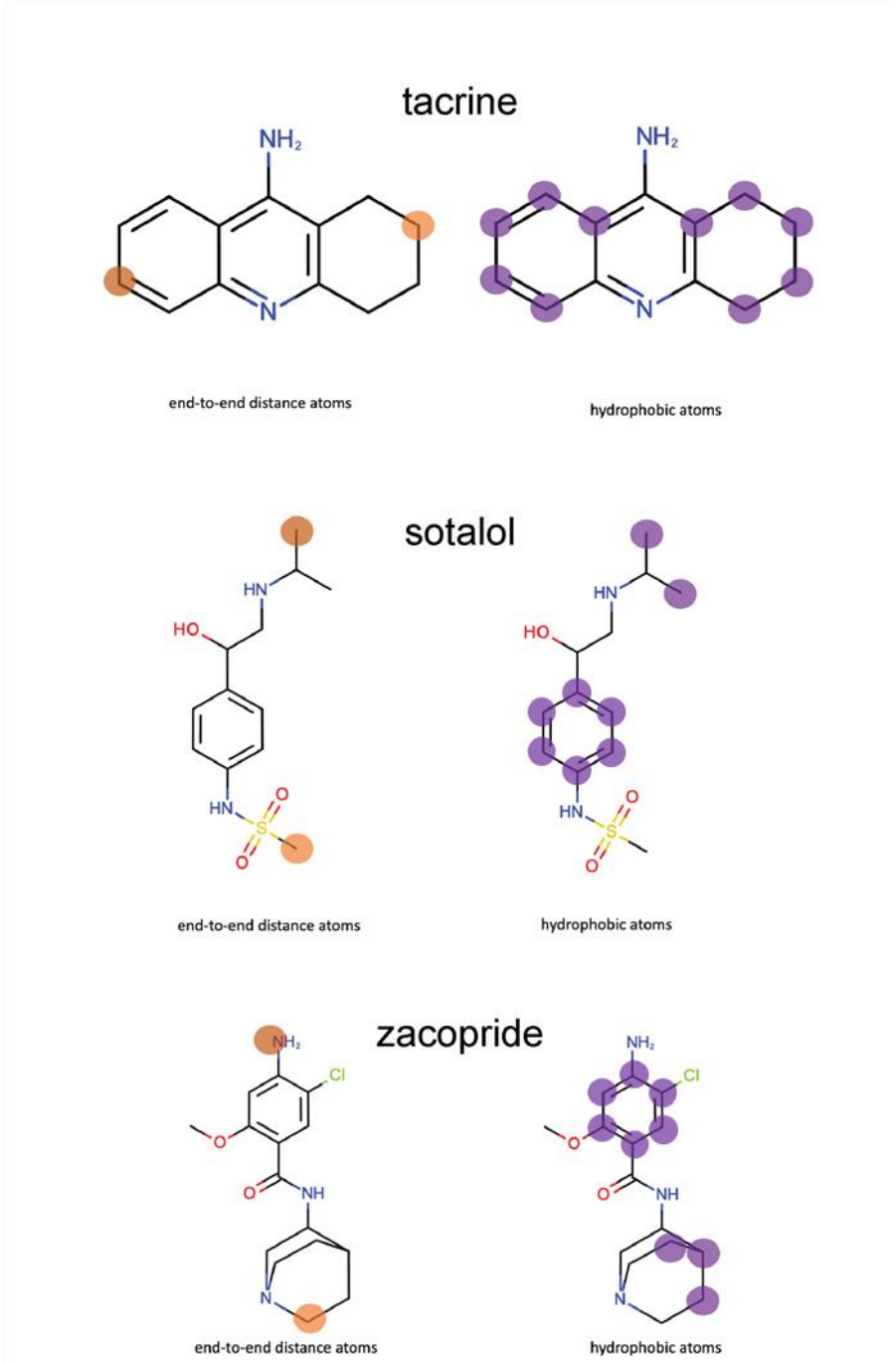

Figure S6. Chemical structures of tacrine, sotalol, and zacopride. Atoms that were chosen to calculate the end-to-end distances were marked by orange circles, and the hydrophobic carbons were marked by purple circles.

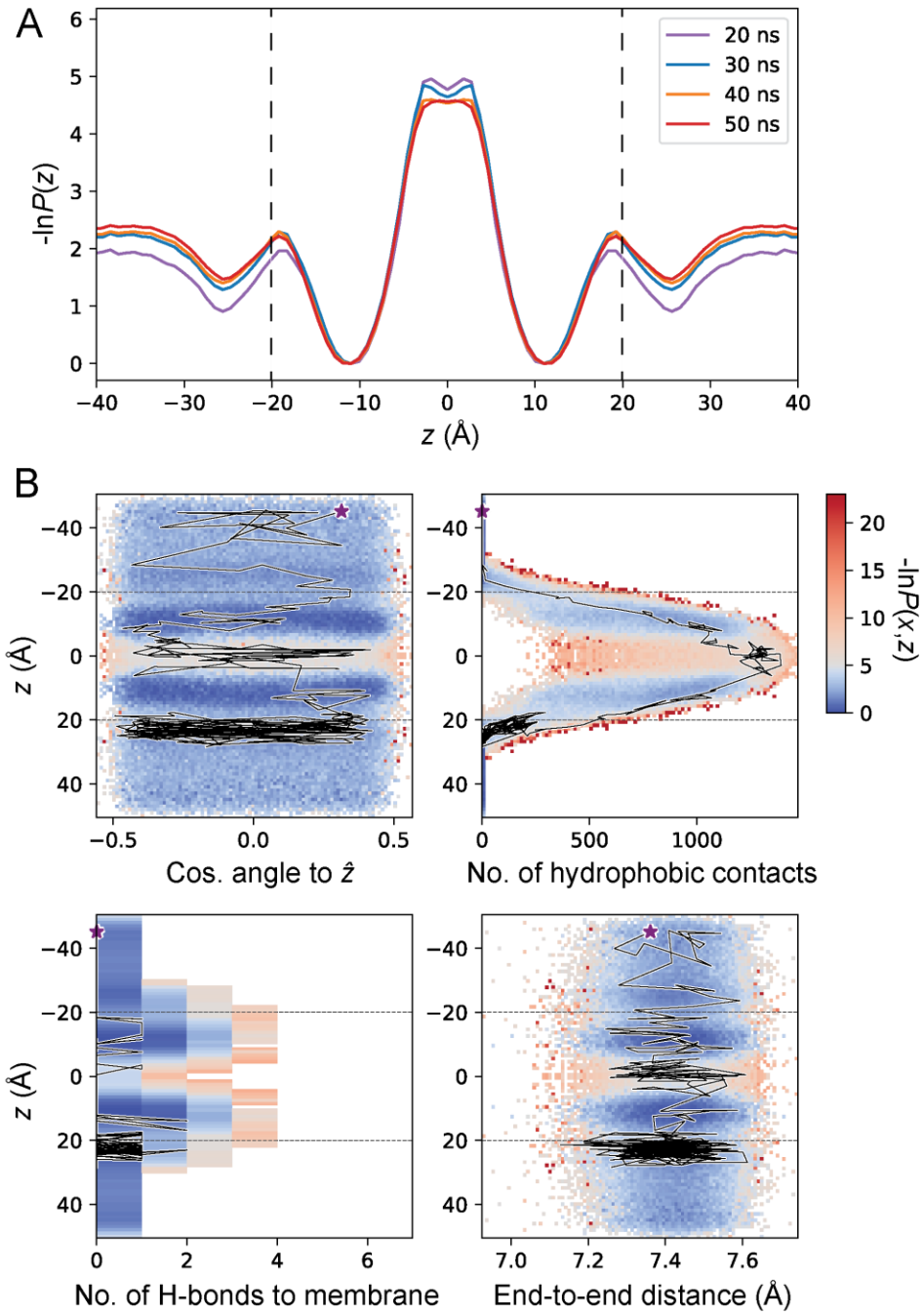

Figure S7. Free energy profiles along the lipid normal ($\hat{z}$) and auxiliary coordinates for tacrine using the MAB scheme and reweighting WE protocol (MAB + WESS). See Figure 3 legend for details.

Table S1. Predicted and experimentally determined permeabilities.

Compound	MAB Adaptive binning	WESS Reweight-ing	Platform	Predicted Log P_m (cm/s)	Expt. Log P_m (cm/s)
Tacrine			GPU	-5.54 ± 0.13	-4.64, -5.03 ± 0.2,
		×	GPU	-3.23 ± 0.09	
	×		GPU	-6.96 ± 0.16	
	×	×	GPU	-4.27 ± 0.24	
	×	×	CPU	-5.20 ± 0.28	
Sotalol	×	×	GPU	-5.32 ± 0.22	-6.02, -5.58 (TtoB), -6.74 (BtoT)
Zacopride	×	×	GPU	-6.35 ± 0.22	-5.23